Continued Development of the Look-up-table (LUT) Methodology For Interpretation of Remotely Sensed Ocean Color Data

W. Paul Bissett
Florida Environmental Research Institute
10500 University Center Dr.
Suite 140
Tampa, FL 33612 USA
phone: (813) 866-3374 x102 fax: (813) 977-8057 email: pbissett@feriweb.org

Award Number: N000140610370
http://www.FERIweb.org
http://www.onr.navy.mil/sci_tech/32/322/ocean_optics_biology.asp

LONG-TERM GOAL

The overall goal of this work is to refine and validate a spectrum-matching and look-up-table (LUT) technique for rapidly and accurately inverting remotely sensed hyperspectral reflectances to extract environmental information such as water-column optical properties, bathymetry, and bottom classification.

OBJECTIVES

My colleagues and I are developing and evaluating new techniques for the extraction of environmental information including water-column inherent optical properties (IOPs), shallow-water bathymetry, and bottom classification from remotely-sensed hyperspectral ocean-color spectra. We address the need for rapid, automated interpretation of hyperspectral imagery. The research issues center on development and evaluation of spectrum-matching algorithms, including the generation of confidence metrics for the retrieved information. Dr. Curtis D. Mobley at Sequoia Scientific, Inc., is leading this effort and he is the author of this report.

APPROACH

The LUT methodology is based on a spectrum-matching and look-up-table approach in which the measured remote-sensing reflectance spectrum is compared with a large database of spectra corresponding to known water, bottom, and external environmental conditions. The water and bottom conditions of the water body where the spectrum was measured are then taken to be the same as the conditions corresponding to the database spectrum that most closely matches (by some chosen metric) the measured spectrum.

In previous LUT work, we have simultaneously retrieved water column IOPs, bottom depth, and bottom classification at each pixel from the remote-sensing reflectance R_{rs} spectra. This is much to ask from a simple R_{rs} spectrum, but we have shown that all of this information is uniquely contained in hyperspectral reflectance signatures and that the information can be extracted with considerable accuracy (Mobley et al., 2005; Mobley and Lesser, 2007).

Report Documentation Page

Form Approved
OMB No. 0704-0188

1. REPORT DATE	2. REPORT TYPE	3. DATES COVERED
2008		**00-00-2008 to 00-00-2008**

4. TITLE AND SUBTITLE	5a. CONTRACT NUMBER
Continued Development of the Look-up-table (LUT) Methodology For Interpretation of Remotely Sensed Ocean Color Data	5b. GRANT NUMBER
	5c. PROGRAM ELEMENT NUMBER
6. AUTHOR(S)	5d. PROJECT NUMBER
	5e. TASK NUMBER
	5f. WORK UNIT NUMBER
7. PERFORMING ORGANIZATION NAME(S) AND ADDRESS(ES) **Florida Environmental Research Institute,10500 University Center Dr.,Tampa,FL,33612**	8. PERFORMING ORGANIZATION REPORT NUMBER
9. SPONSORING/MONITORING AGENCY NAME(S) AND ADDRESS(ES)	10. SPONSOR/MONITOR'S ACRONYM(S)
	11. SPONSOR/MONITOR'S REPORT NUMBER(S)

12. DISTRIBUTION/AVAILABILITY STATEMENT
Approved for public release; distribution unlimited

13. SUPPLEMENTARY NOTES

14. ABSTRACT

15. SUBJECT TERMS

16. SECURITY CLASSIFICATION OF:			17. LIMITATION OF ABSTRACT	18. NUMBER OF PAGES	19a. NAME OF RESPONSIBLE PERSON
a. REPORT **unclassified**	b. ABSTRACT **unclassified**	c. THIS PAGE **unclassified**	**Same as Report (SAR)**	**10**	

Our initial work considered only retrievals based on the closest matching LUT database R_{rs} spectrum to a given image spectrum. However, exactly which database spectrum most closely matches the image spectrum can be influenced by noise in the image spectrum. Therefore, last year's work considered retrievals based not just on the closest-fitting database spectrum, but on the *k* closest fitting spectra. Use of the *k* (typically $k = 30$ to 50) closest spectra not only allows various statistical estimates of the retrieved information (depth, bottom type, etc), but also provides statistically based error bars and confidence statements about the retrieved information.

This year's work continued the process of examining various ways to improve retrievals, in particular by taking advantage of spatial correlations in the environmental variables from one pixel to the next. We also examined the errors in the LUT R_{rs} database generation associated with the use of unpolarized (scalar) radiative transfer calculations (using a special version of HydroLight), compared to exact (but very time consuming) calculations that included polarization.

WORK COMPLETED

Previous retrievals (e.g., Mobley, et al., 2005; Lesser and Mobley, 2007) have processed each image pixel independently of its neighbors. However, there is usually a strong spatial correlation in neighboring pixels because water depth and IOPs, and bottom type, often do not change greatly from one pixel to the next (i.e., on a scale of one to a few meters). We therefore examined various ways to spatially smooth the input R_{rs} spectra (before processing) and/or the output environmental values (after processing) to take advantage of spatial similarities in small blocks of pixels (e.g., 3x3 or 5x5 blocks centered on the pixel of interest).

Colleagues Y. You, G. Kattawar, and B. Hauss and Mobley also did detailed comparison runs using coupled ocean-atmosphere vector radiative transfer codes available to You and Kattawar to quantify the errors resulting in upwelling atmospheric radiances and in R_{rs} when the ocean and the atmosphere are modeled (1) using polarized (vector) radiative transfer (RT) theory, (2) unpolarized (scalar) RT, and (3) a vector atmosphere but a scalar ocean. We considered upwelling radiances just above the sea surface (relevant to R_{rs} spectra measured for ground truth and to the generation of the LUT database), at 3,000 m altitude (relevant to airborne remote sensing platforms as employed in our work), and at the top of the atmosphere (relevant to satellite remote sensing). A paper on those results has been submitted to *Applied Optics* (You, et al., 2008).

In addition to the work discussed above, M. Lesser and Mobely published (Lesser and Mobley, 2007) a detailed analysis of LUT depth and bottom classification retrievals in the localized area of Horseshoe Reef, Lee Stocking Island, Bahamas, for which bottom classification information was available from underwater transects by divers. The LUT results were in good agreement with ground truth for percent coverage of sediments, corals, and mixed bottom types over the reef.

Finally, a patent titled "Spectral Imaging System" was granted to the collaborators on this LUT work. That patent covers various aspects of both image acquisition hardware and image analysis software, including the LUT methodology.

RESULTS

We investigated two types of spatial smoothing. The first smoothes the image R_{rs} spectra before performing the LUT matching, and the second smoothes the retrieved depths (or other quantities, such

as IOPs or bottom reflectances) after performing the LUT matching. The two types of smoothing can be done independently or in combination, and in combination with the kNN analysis techniques investigated last year.

To spatially smooth an R_{rs} spectrum, we considered an $n \times n$ block of pixels centered on the pixel of interest, with $n = 1, 3, 5, \ldots$ ($n = 1$ corresponds to no spatial smoothing). Let $R_{rs}(i,j,\lambda)$ be the image spectrum at pixel (i,j). We reasoned that we want to average the "good" spectra in the $n \times n$ block of pixels centered on (i,j), but we do not want to include any anomalously large or small "bad" spectra that might be contaminated by sun glint or whitecaps (or other causes). For $n = 3$, we have a 3×3 block of 9 pixels centered on (i,j). To help eliminate anomalously large or small "bad" spectra, we discarded the highest and smallest values of the 9 spectra at each wavelength, and averaged the remaining 7 values. For $n = 5$, we have a 5×5 block of 25 pixels. In that case, we discard the highest 2 and lowest 2 values, and averaged the remaining 21 values. If some of the pixels are flagged as land, clouds, or whitecaps, or if (i,j) is next to the image boundary, there are fewer than n^2 valid pixels. We then have a reduced number of pixels to work with, but the procedure is the same: discard the highest and lowest values and average the remaining values. The original $R_{rs}(i,j,\lambda)$ is then replaced by the average spectrum computed from the $n \times n$ block of pixels. Note that this algorithm is applied independently at each wavelength. Thus the particular spectra that are eliminated at one wavelength may or may not be the spectra that are eliminated at another wavelength.

To smooth the retrieved depths we again consider $n \times n$ blocks of pixels. Now, however, we do not discard the high or low values of the retrieved depths before averaging. The reason is that when doing kNN matching, the kNN algorithm already, by its very nature, may have omitted the high or low values, or done some other sort of filtering or averaging of the k retrieved depths at each pixel. We therefore omit only pixels in the $n \times n$ block that are flagged as invalid (land, cloud, etc), and we then average the remaining (usually n^2) depths to obtain the spatially smoothed depth for the pixel at the center of the $n \times n$ block.

Figure 1 shows a 3D perspective plot of the bathymetry near Lee Stocking Island (LSI), Bahamas; LSI is the gray area at the upper left of the image. This figure shows the results for no spatial smoothing ($n = 1$) of either the input R_{rs} spectra or of the retrieved depths, and the closest-matching ($k = 1$) database spectrum was used. This baseline retrieval corresponds to the retrievals shown in Mobley et al. (2005). The pixel-to-pixel variability of the retrieved depths is quite apparent. Figure 2 shows the quantitative comparison of the retrieved vs. acoustically measured depths for the pixels where an acoustic depth was available. We see that the average retrieved depth is about 7% (0.4 m) too shallow, with a standard deviation of 1.2 m between retrieved and measured depths. 68% of the pixels have retrieved depths within ±1 m of the acoustic depth, and 87% are within ±25% of the acoustic value.

Figures 3 and 4 show the corresponding results from a combination of kNN matching and spatial smoothing. Figure 3 shows the 3D plot of retrieved depths when (1) the input R_{rs} spectra are smoothed using a 5x5 spatial grid, (2) the retrieved depths are then obtained as the median of the closest $k = 30$ spectra, and (3) the retrieved depths are then smoothed using a 5x5 grid. The final retrieved depths are now clearly much smoother from pixel to pixel. Figure 4 shows the quantitative errors for Fig. 3. We now see that the average error is only 0.8% (0.04 m) too shallow, with a standard deviation of 0.9 m. Now 76% of the all pixels are within ±1 m of the acoustic value, and 95% of all pixels are within ±25% of the acoustic value.

The combination of spatial smoothing and kNN analysis clearly improves the average accuracy of the retrieved depths and reduces the pixel-to-pixel variability.

The LUT R_{rs} database is generated by a special version of the HydroLight radiative transfer model, which solves the unpolarized (scalar) radiative transfer equation (RTE). Omission of polarization in the database generation leads to some error in the computed R_{rs} spectra. We therefore examined (with the assistance of Y. You, G. Kattawar, and B. Hauss) the nature of these errors through numerical simulations using coupled ocean-atmosphere radiative transfer codes that solve the polarized (vector) RTE. We evaluated the errors in upwelling radiances due to the omission of polarization in either the ocean or atmosphere for a wide range of oceanic and atmospheric conditions, sun and viewing geometries, and wavelengths from 415 to 865 nm. We considered the errors at the sea surface (relevant to R_{rs} computation for the LUT database and to sea truth measurements used for validation of remote sensing imagery), at 3,000 m altitude (relevant to airborne remote sensing platforms), and at the top of the atmosphere (relevant to satellite ocean color remote sensing).

Figures 5 and 6 illustrate the errors in the water-leaving radiance when both the ocean and the atmosphere are modeled with the unpolarized RTE (left panels), and when the atmosphere and sea-surface reflectance are polarized but the ocean is unpolarized (right panels). It is seen that the errors in the water-leaving radiance are less than 3% when the underwater RT calculations are performed using the scalar RTE (as is done in HydroLight), whether or not the atmospheric calculations are performed with scalar or vector codes. Surface waves have almost no effect on these errors compared to the effects of sun and viewing geometry and water and atmospheric conditions. These results justify the use of the computationally efficient HydroLight scalar ocean radiative transfer model to computed R_{rs} spectra for the LUT database, so long as errors up to 3% can be tolerated. This is indeed the case for most ocean color remote sensing, since the errors owing to imperfect sensor radiometric calibration and atmospheric correction of the imagery are often greater. The results for 3,000 m and top-of-atmosphere comparisons, and for other parameter values, can be found in the You et al. (2008) paper.

IMPACT/APPLICATION

The problem of extracting environmental information from remotely sensed ocean color spectra is fundamental to a wide range of Navy needs as well as to basic science and ecosystem monitoring and management problems. Extraction of bathymetry and bottom classification is especially valuable for planning military operations in denied access areas. The ability to simultaneously generate error estimates on retrieved values is often equally important to the ability to retrieve the environmental information itself; this can be accomplished using the kNN techniques reported last year. The ability to use spatial correlations to filter anomalous values and improve retrievals, as developed this year, greatly enhances the reliability of the retrievals.

TRANSITIONS

Various databases of water IOPs, bottom reflectances, and the corresponding R_{rs} spectra, along with the specialized Hydrolight code and spectrum-matching algorithms have been transitioned to Dr. Paul Bissett at the Florida Environmental Research Institute for processing his extensive collection of SAMPSON imagery acquired in coastal California waters, and for use in comparisons of LUT and LIDAR bathymetry.

RELATED PROJECTS

This work is being conducted in conjunction with Dr. Curtis D. Mobley at Sequoia Scientific, Inc., who is separately funded for this collaboration. These techniques developed here are now being applied to imagery of Australian coastal waters in a comparison of several different hyperspectral remote sensing algorithms for a variety of environments. That comparison study is being led by A. Dekker of CSIRO.

REFERENCES

Mobley, C. D., L. K. Sundman, C. O. Davis, T. V. Downes, R. A. Leathers, M. J. Montes, J. H. Bowles, W. P. Bissett, D. D. R. Kohler, R. P. Reid, E. M. Louchard, and A. Gleason, 2005. Interpretation of hyperspectral remote-sensing imagery via spectrum matching and look-up tables. *Applied Optics* 44(17), 3576-3592.

Lesser, M. P. and C. D. Mobley, 2007. Bathymetry, optical properties, and benthic classification of coral reefs using hyperspectral remote sensing imagery. *Coral Reefs*, 26: 819-829.

You, Y., G. W. Kattawar, C. D. Mobley, and B. Hauss, 2008. Polarization effects on upwelling marine atmospheric radiances. *Applied Optics* (submitted).

PUBLICATIONS

Lesser, M. P. and C. D. Mobley, 2007. Bathymetry, optical properties, and benthic classification of coral reefs using hyperspectral remote sensing imagery. *Coral Reefs*, 26: 819-829 [Refereed, published]

You, Y., G. W. Kattawar, C. D. Mobley, and B. Hauss, 2008. Polarization effects on upwelling marine atmospheric radiances. *Applied Optics* [Refereed, submitted]

PATENT

U. S. Patent 7369229 titled “Spectral Imaging System” was granted on 06 May 2008 to W. P. Bissett III, D. D. R. Kohler, R. G. Steward, and C. D. Mobley. This patent covers various aspects of both the hardward and software used for hyperspectral image acquisition and analysis, including the LUT methodology. [Granted]

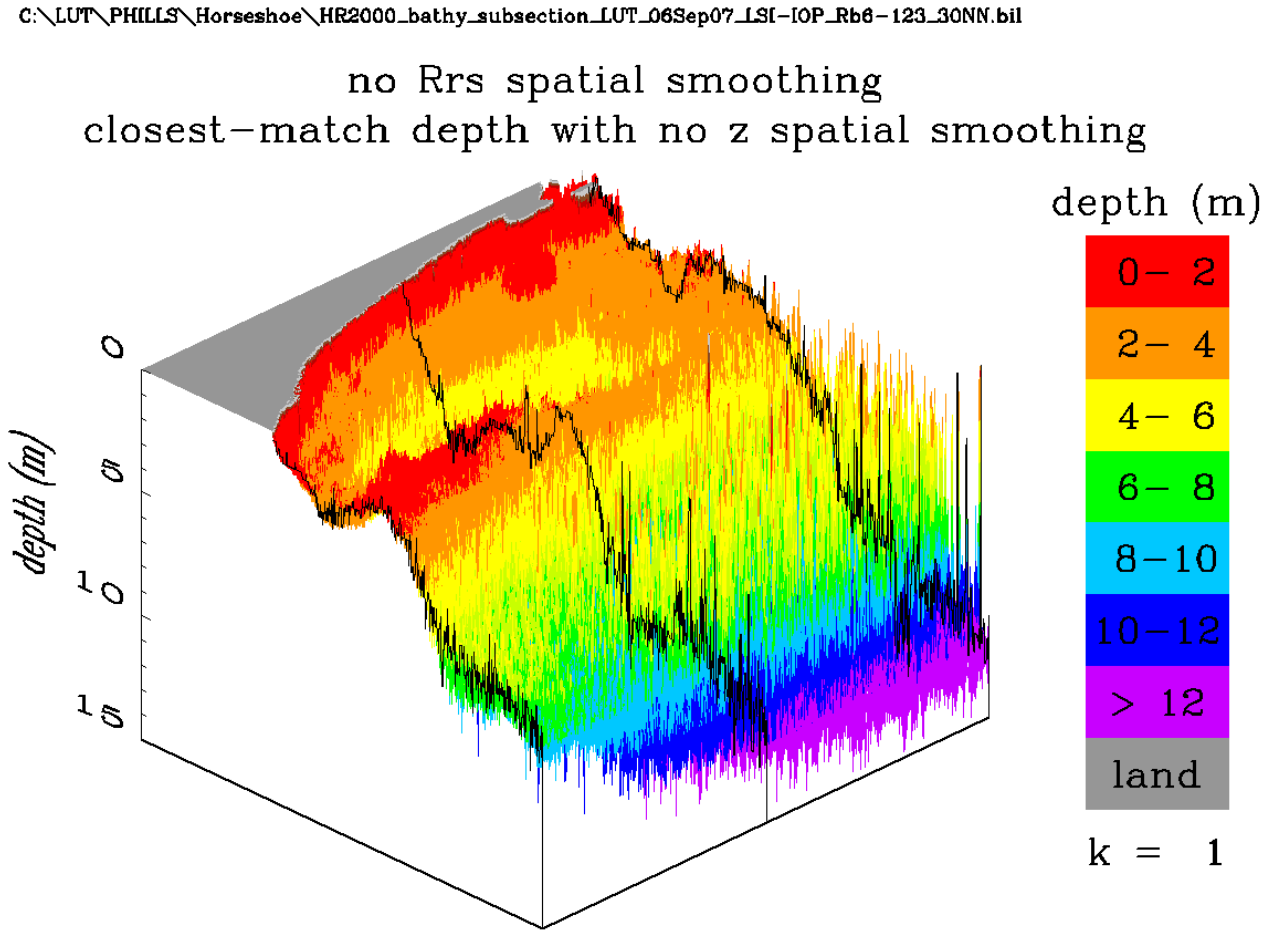

Fig. 1. LUT-retrieved depths plotted as a 3D surface and viewed in perspective. Lee Stocking Island is the gray area at the upper left. The pixel-to-pixel spikiness or variability of the depth retrievals is quite apparent. The three black lines show the depths at each pixel along selected transects of the area. The corresponding quantitative comparison of LUT-retrieved vs. acoustic-measured depths is shown in Fig. 2. [The figure shows a 3D perspective plot of retrieved depths at each pixel with the depth color coded: red is 0-2 m to purple is >12m deep.]

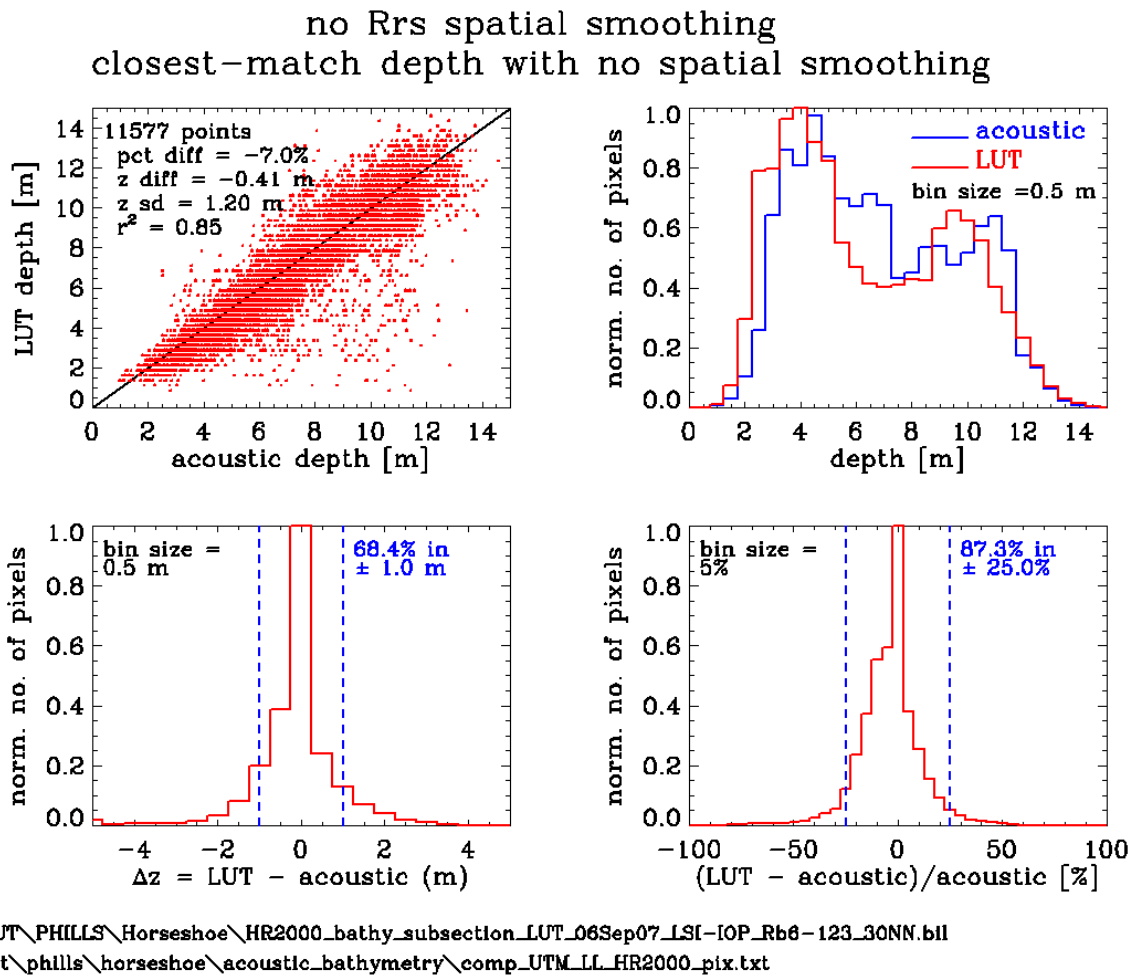

Fig. 2. LUT vs. acoustic depths for the no-smoothing, closest-match retrieval of Fig. 1, displayed in various ways. [The figure compares the differences in retrieved and measured depths in four different ways.]

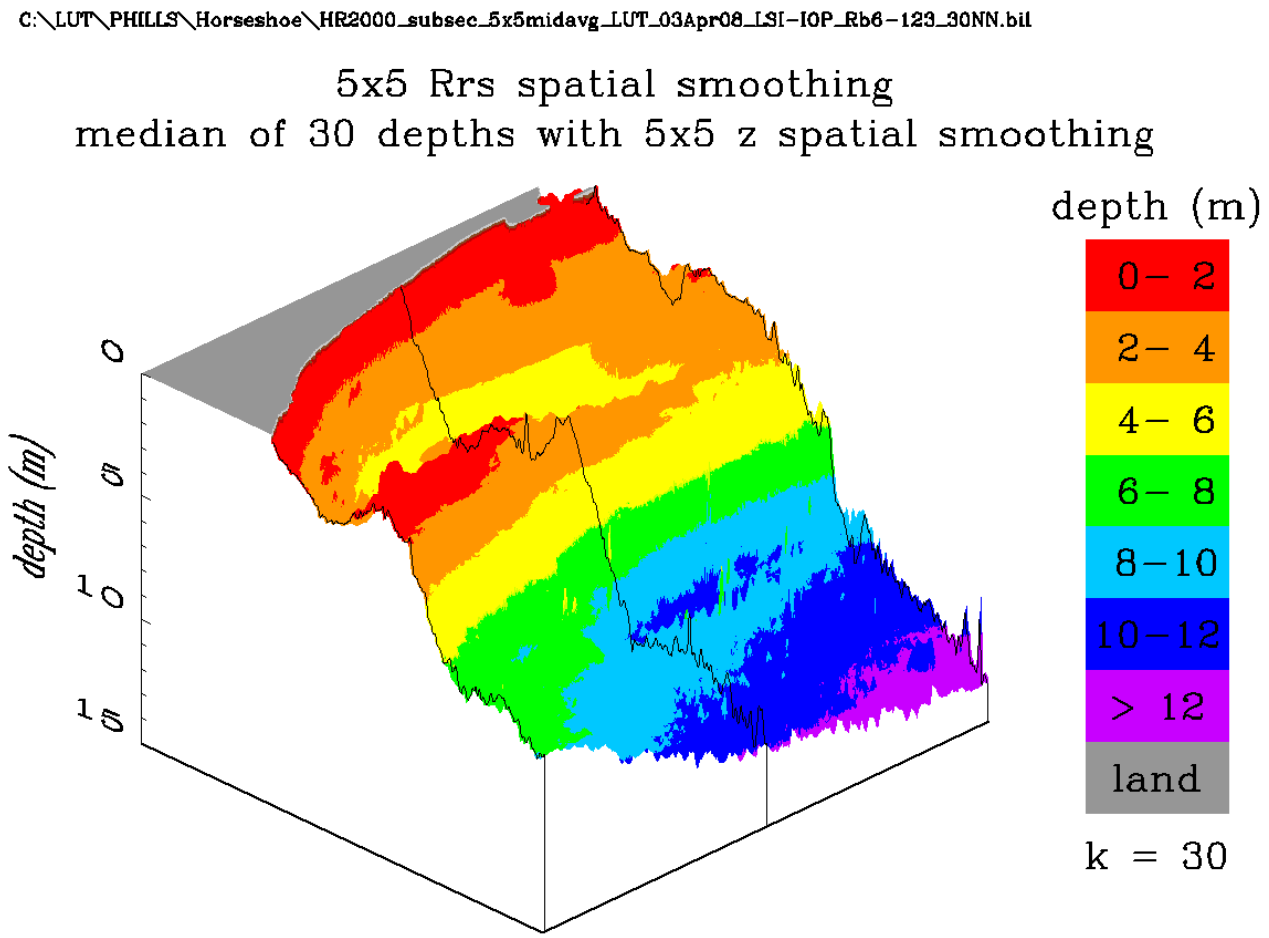

Fig. 3. The 3D perspective of the retrieved depths when 5x5 spatial smoothing in performed on both the input R_{rs} spectra and the output depths, and the retrieved depth is the median of k = 30 closest matching spectra. The pixel-to-pixel spikiness or variability of the depth retrievals greatly reduced compared to what is seen in Fig. 1. The corresponding quantitative comparison of LUT-retrieved vs. acoustic-measured depths is shown in Fig. 4. [The figure shows a 3D perspective plot of retrieved depths at each pixel with the depth color coded.]

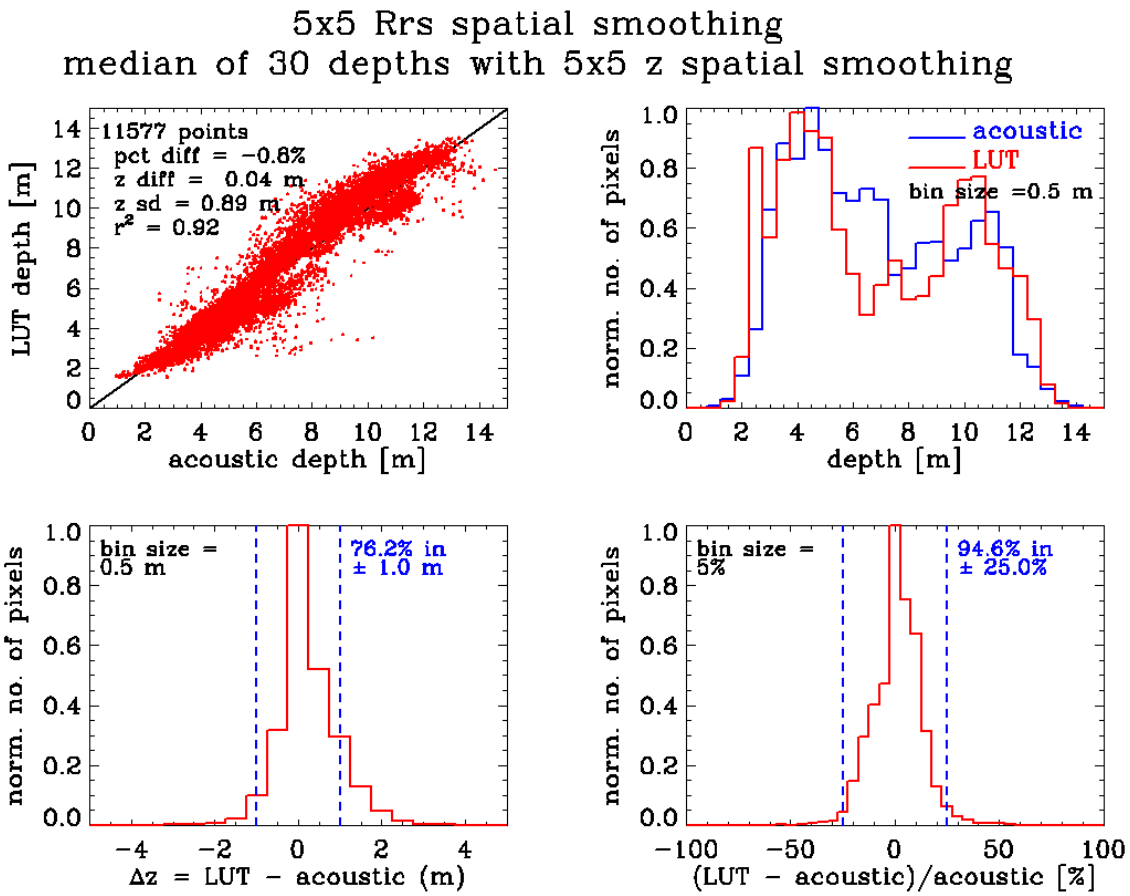

C:\LUT\PHILLS\Horseshoe\HR2000_subsec_5x5midavg_LUT_03Apr08_LSI-IOP_Rb6-123_30NN.bil
c:\lut\phills\horseshoe\acoustic_bathymetry\comp_UTM_LL_HR2000_pix.txt

Fig. 4. LUT vs. acoustic depths for the smoothed kNN retrieval of Fig. 3, displayed in various ways. Compare with Fig. 2. [The figure compares the differences in retrieved and measured depths in four different ways.]

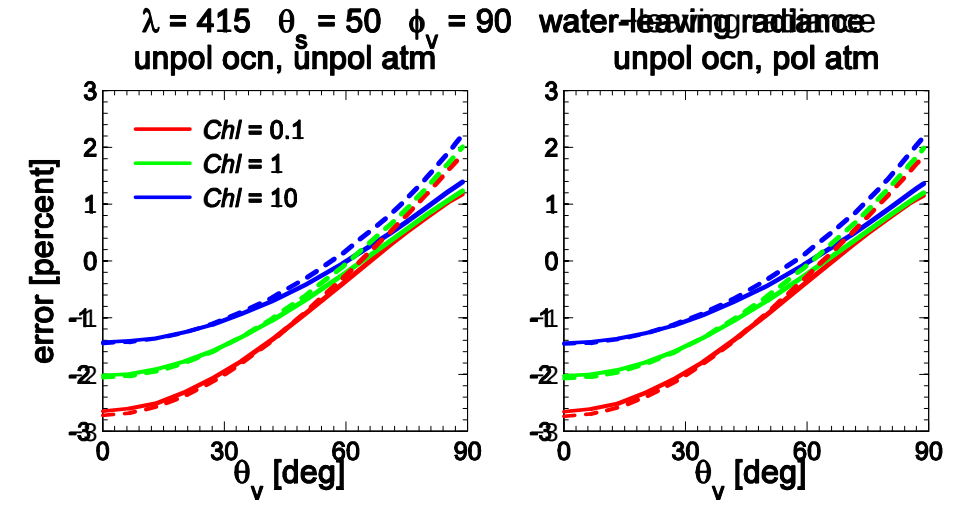

Fig. 5. Errors in the water-leaving radiance just above the sea surface for low (Chl = 0.1 mg m^{-3}), medium (Chl = 1) and high (Chl = 10) chlorophyll concentrations. This figure is for 415 nm, sun at a 50 deg zenith angle, viewing at right angles to the sun (ϕ_v = 90), from nadir (θ_v = 0) to horizon. Solid lines are for a clear atmosphere, dashed lines are for a very hazy atmosphere. [Curves show errors of less than ±3% in the water-leaving radiance for a wide range of chlorophyll concentrations.]

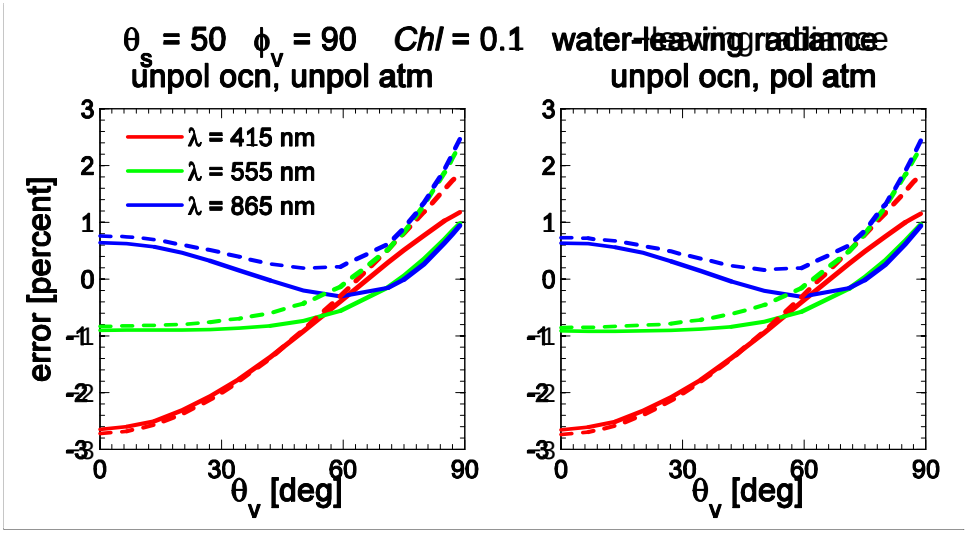

Fig. 6. Errors in the water-leaving radiance just above the sea surface for wavelengths of 415, 555, and 865 nm. low (Chl = 0.1 mg m^{-3}), medium (Chl = 1) and high (Chl = 10) chlorophyll concentrations. This figure is for a low chlorophyll concentration of 0.1 mg m^{-3}, sun at a 50 deg zenith angle, viewing at right angles to the sun (ϕ_v = 90), from nadir (θ_v = 0) to horizon. Solid lines are for a clear atmosphere, dashed lines are for a very hazy atmosphere. [Curves show errors of less than ±3% in the water-leaving radiance for a wide range of wavelengths.]